23rd International Conference on Renewable Energies and Power Quality (ICREPQ'25)
Tenerife (Spain), 25th to 27th June 2025
ISBN-13: 978-84-09-66511-2

Experimental $LiFePO_4$ Battery Cycling System. Analysis and Simulation of a stand-alone/on-grid Photovoltaic Applications.

J.S. Artal-Sevil, J.M. Lujano-Rojas, R. Dufo-López, J.L. Bernal-Agustín, J.A. Tejero-Gómez

Department of Electrical Engineering.
Higher Technical School of Industrial Engineering.
University of Zaragoza.
Campus Río Ebro – Zaragoza 50018 (Spain).
email: {jsartal; lujano.juan; rdufo; jlbernal; jatejero}@unizar.es

Abstract. This paper presents the design, modeling, and validation of an experimental $LiFePO_4$ battery cycling system applied to stand-alone and on-grid photovoltaic (PV) scenarios. A comprehensive analysis of battery behaviour -including key parameters such as *SOC*, *SOH*, *DOD*, and internal resistance- is conducted to highlight the advantages of $LiFePO_4$ chemistry in terms of safety, thermal stability, and cycle life. The charge/discharge dynamics are governed by the CCCV protocol, with detailed insights into voltage plateau behaviour, degradation mechanisms, and second-life reuse potential. The proposed experimental platform integrates a programmable power supply, active load, and full monitoring system to simulate real irradiance and consumption profiles with high temporal resolution. Results from the test-bench validate the accurate tracking of *SOC*, power flow optimization, and effective battery cycling under fluctuating PV conditions. Colour-map diagrams and hourly data analyses demonstrate the system's capacity to balance generation, storage, and consumption, ensuring reliability and autonomy. The setup also enables the modeling of thermal and electrical behaviour at minute-level resolution, offering a valuable tool for the simulation and development of distributed PV-battery storage systems. The energy balance analysis, based on minutely power data, confirms the model's accuracy in simulating real-world PV-battery interactions.

Keywords. Battery Cycling System, $LiFePO_4$ Battery, Battery charge/discharge, *SOC/SOH* estimation, *BMS*, stand-alone/on-grid Photovoltaic Power System.

1. Introduction

Lithium iron phosphate ($LiFePO_4$) batteries have emerged as one of the most promising storage technologies in renewable energy applications due to their high thermal stability, long cycle life, and enhanced safety characteristics. Compared to other lithium-based chemistries, $LiFePO_4$ cells exhibit superior resistance to overheating and chemical degradation, making them particularly suitable for integration in photovoltaic (PV) systems [1], whether in stand-alone configurations or hybrid on-grid setups. As renewable energy deployment continues to grow, the need for robust and efficient energy storage solutions becomes increasingly critical, especially for ensuring power reliability and mitigating the intermittency of solar resources [2].

A difficulty in the integration of battery systems lies in the accurate monitoring and management of fundamental performance indicators, such as the state of charge (*SOC*), state of health (*SOH*), depth of discharge (*DOD*), effective capacity, and internal resistance [3]. These parameters are essential not only for optimizing energy use and prolonging battery life but also for developing control strategies that adapt to variable environmental conditions and load demands. However, obtaining reliable estimations of these parameters under real operating conditions remains complex due to the influence of nonlinear behaviours, temperature effects, current rates, or electrochemical aging. This study presents the design and implementation of an experimental cycling system tailored to $LiFePO_4$ batteries, integrated within a hybrid photovoltaic laboratory setup.

Fig. 1. Batteries and inverters associated with a stand-alone solar photovoltaic system. Barbastro (Zaragoza, Spain).

2. $LiFePO_4$ Batteries: Parameters, Models, Definitions, and Considerations

The performance and longevity of lithium-based batteries, particularly $LiFePO_4$ (Lithium Iron Phosphate), depend critically on several characteristic parameters. Understanding and quantifying these parameters -namely the state of charge (*SOC*), state of health (*SOH*), depth of discharge (*DOD*), and capacity- is essential for the optimal design, monitoring, and operation of energy storage systems, especially in hybrid and photovoltaic (PV) applications.

A. State of Charge (SOC)

The *SOC* represents the ratio between the current charge available in the battery and its nominal capacity. It is analogous to a fuel gauge, indicating the remaining energy. The basic definition is:

$$SOC(t) = SOC(t_0) - \frac{1}{C_{nom}} \int_{t_0}^{t} I(t)dt \quad (1)$$

where C_{nom} is the nominal capacity in Ah, and *I(t)* is the battery current (positive during discharge, negative during charge). Accurate *SOC* estimation is non-trivial due to factors such as Coulombic efficiency, temperature variations, and current rate. Methods for *SOC* estimation include Coulomb counting, open-circuit voltage (*OCV*) mapping, Kalman filters, and machine learning techniques in advanced battery management systems (*BMS*).

B. State of Health (SOH)

The *SOH* provides a quantitative measure of battery degradation, representing the aging status relative to a new battery. It is defined as:

$$SOH = \frac{C_{actual}}{C_{rated}} \times 100\% \quad (2)$$

where C_{actual} is the current maximum capacity and C_{rated} is the rated (initial) capacity. *SOH* also includes degradation of internal resistance, self-discharge rate, and thermal stability. A comprehensive *SOH* evaluation may require electrochemical impedance spectroscopy (EIS), differential capacity analysis, or thermal modeling. When *SOH* drops below 80%, most manufacturers recommend battery replacement for critical applications.

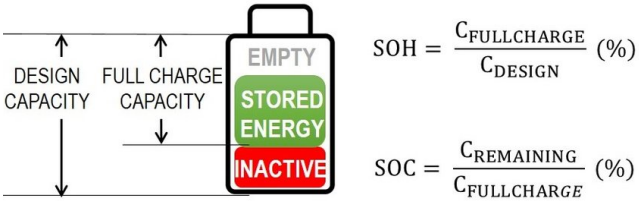

Fig. 2. Simplified representation of battery *SOH* and *SOC* metrics. *SOH* quantifies battery capacity degradation and impacts on the estimation of *SOC*.

C. Depth of Discharge (DOD)

DOD quantifies how much of the battery's capacity has been used during a discharge cycle:

$$DOD = 100\% - SOC \quad (3)$$

High *DOD* values correlate with faster aging, especially in lithium-based chemistries. Partial cycling (e.g., operating between 30–80% *SOC*) significantly extends battery life, a strategy frequently applied in PV and off-grid systems. *DOD* impacts the cycle life exponentially; empirical models suggest an inverse power law relation between cycle life and *DOD*.

D. Battery Capacity

Capacity denotes the total electric charge a battery can deliver at rated conditions and is expressed in Ah or Wh:

$$C = \int_0^T I(t)dt \quad (4)$$

Real capacity depends on discharge rate (C-rate), temperature, and aging. For instance, high C-rates reduce the usable capacity due to increased internal resistance and heat generation. The capacity fade over time follows complex aging laws influenced by solid electrolyte interphase (SEI) layer growth, lithium plating, and structural fatigue of electrodes.

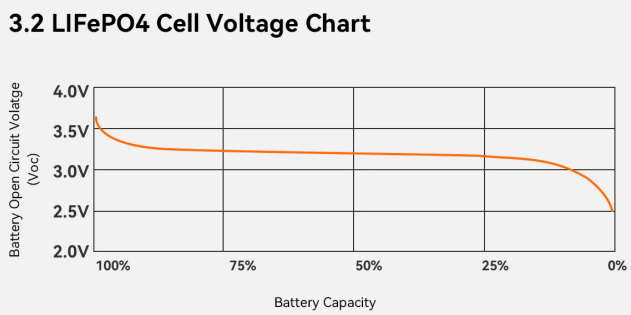

Fig. 3. A voltage graph is commonly used to monitor the state of charge (*SOC*) of a $LiFePO_4$ battery.

E. Internal Resistance (R_{int})

The internal resistance R_{int} affects energy efficiency and thermal behaviour. It increases with battery aging and is influenced by temperature, state of charge, and current load. A simplified model is:

$$v_{bat} = OCV(SOC) - I \cdot R_{int} \quad (5)$$

where v_{bat} is the terminal voltage. In dynamic modeling, the Randles or Thevenin equivalent circuits are used to describe transient voltage behaviour under load.

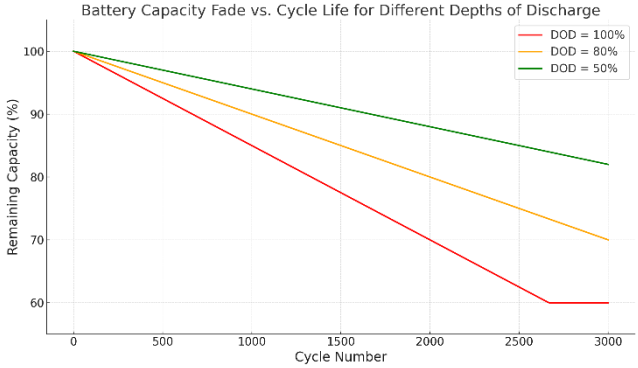

Fig. 4. Battery capacity degradation as a function of the number of cycles for different depth of discharge (*DOD*) values.

F. Technological Advantages

$LiFePO_4$ batteries offer high thermal and chemical stability, low self-discharge rates (<3% per month), and a long cycle life (>2000 cycles at 80% *DOD*). They are intrinsically safer than other lithium chemistries due to their robust cathode material and resistance to thermal runaway. Their flat discharge voltage profile and excellent cycle performance make them ideal for renewable energy integration and standalone PV systems.

G. Limitations and Operational Recommendations

- Thermal Management: Lithium batteries operate optimally between 15–35°C. High temperatures accelerate degradation, while low temperatures impair power output and charging efficiency.
- Cycle Life Optimization: Avoiding full 100% *DOD* and operating within a moderate *SOC* window (e.g., 20–80%) can double or triple cycle life in $LiFePO_4$ cells.

- Charge Protocols: The CC-CV (constant current–constant voltage) charging method is standard. Overcharging (>4.2V per cell) or deep discharging (<2.0V per cell) should be avoided to prevent irreversible damage.
- Storage Practices: Long-term storage at 40–60% *SOC* and cool environments minimizes capacity loss.

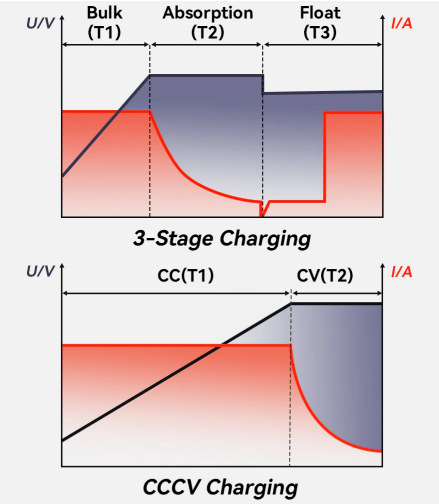

Fig. 5. Simplified representation of battery *SOH* and *SOC* metrics. *SOH* quantifies battery capacity degradation and impacts on the estimation of *SOC*.

3. $LiFePO_4$ Batteries: charge/discharge

Lithium iron phosphate ($LiFePO_4$) batteries have emerged as a leading choice in stationary and mobile energy storage systems due to their superior thermal stability, extended cycle life, and favorable electrochemical properties. The charge-discharge process of $LiFePO_4$ cells is governed by the constant current–constant voltage (CCCV) algorithm, which is typically divided into two principal phases. In the constant current (CC) phase, the battery is charged with a predefined current -usually between 0.2C and 1C- while the terminal voltage increases progressively. This stage continues until the cell voltage reaches a target threshold, generally around +3.65V for $LiFePO_4$ chemistry. During this phase, lithium ions are intercalated into the cathode material, and the internal electrochemical potential gradually rises. Once the cut-off voltage is reached, the charger transitions to the constant voltage (CV) phase, during which the voltage is held fixed and the charging current naturally tapers off as the cell approaches full saturation. The cut-off current at which the charging process is typically terminated is around 0.01C, ensuring minimal overcharge and extending the cell's cycle life.

The voltage plateau observed during charging is notably flat for $LiFePO_4$ cells, which complicates precise *SOC* estimation based solely on terminal voltage. Unlike other lithium-ion chemistries, $LiFePO_4$ does not benefit from trickle charging or float maintenance due to its inherently low self-discharge rate. Additionally, $LiFePO_4$ cells exhibit a narrower operating voltage range (typically +2.5V to +3.65 V per cell), which requires tighter control algorithms and enhanced *BMS* functionality to prevent overcharging or deep discharges. Proper thermal management during both charging and discharging is critical, as cell performance and internal resistance are highly sensitive to temperature variations. Charging should be performed within a safe thermal window, commonly +10°C to +45°C, to avoid lithium plating or electrolyte degradation. Overcharging or charging at sub-zero temperatures may trigger irreversible side reactions, reducing *SOH* and accelerating capacity fade. Therefore, modern $LiFePO_4$ systems rely on advanced battery management systems capable of real-time monitoring of cell voltage, current, and temperature to maintain safe operating conditions and prolong battery lifespan. The robustness and predictability of the CCCV profile in $LiFePO_4$ chemistry also makes it suitable for second-life applications, where predictable behaviour is essential for performance modeling and integration into heterogeneous storage architectures.

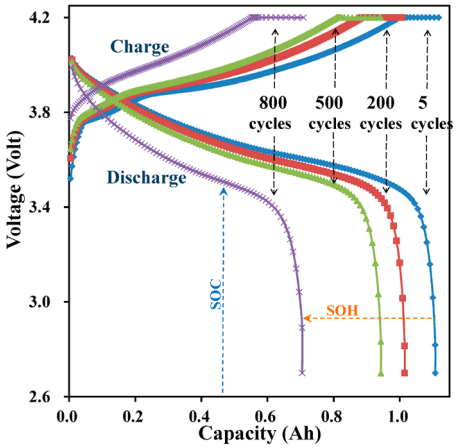

Fig. 6. Example of voltage vs. capacity variations in a battery cell over several charge/discharge cycles.

The degradation of the state of health (*SOH*) in lithium-based batteries, such as $LiFePO_4$, is a multifactorial process driven by both operational and environmental conditions. One of the most significant contributors is cycle aging, wherein each charge-discharge cycle induces mechanical stress and structural changes in the electrode materials, progressively reducing the battery's usable capacity. The depth of discharge (*DOD*) also plays a key role: deeper discharges tend to accelerate capacity fade due to higher lithium-ion mobility and increased intercalation stress. Temperature is another critical factor; elevated temperatures promote side reactions such as electrolyte decomposition and solid electrolyte interphase growth, while low temperatures raise internal resistance and reduce charge acceptance, both leading to faster degradation. Similarly, high charging rates exacerbate thermal stress and lithium plating phenomena, which compromise the structural integrity and safety of the battery.

In addition to these operational factors, chemical degradation mechanisms significantly impact long-term *SOH*. During repetitive cycling, parasitic reactions generate gaseous byproducts and form irreversible compounds that isolate active material, reducing efficiency. Even in the absence of use, calendar aging occurs as a result of time-dependent chemical instabilities within the cell, particularly affecting the SEI layer and electrolyte composition. Over time, these changes manifest as increased impedance, reduced capacity, and thermal instability. Therefore, optimal battery management requires maintaining moderate temperatures, avoiding full charge/discharge cycles, and limiting high-rate charging

events. These strategies not only preserve *SOH* but also enhance the overall reliability and safety of battery-powered systems, especially in stationary applications.

Figure 6 shows a representative voltage versus capacity curve for a lithium-ion cell under selected test cycles. The progressive leftward shift of the discharge curves indicates a reduction in usable capacity, serving as a direct manifestation of battery aging and a key indicator of the state of health (*SOH*). Similarly, the voltage decay profile over time is traditionally associated with the state of charge (*SOC*). However, the instantaneous voltage alone is not a reliable predictor of *SOC*, as the same voltage value may correspond to different *SOC* levels depending on the battery's cycle count *N*. This ambiguity becomes critical when evaluating partially degraded cells or estimating performance without full charge/discharge characterization.

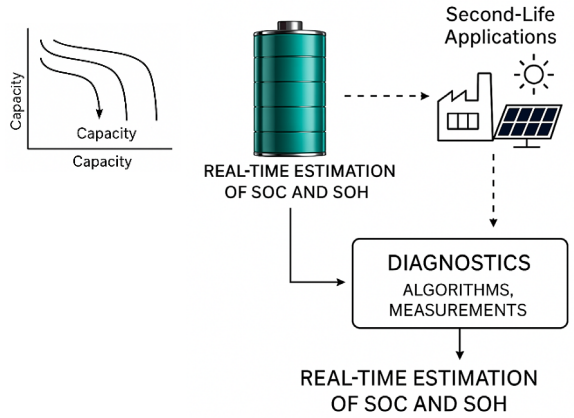

Fig. 7. Complementary diagram showing the idea of reuse + smart diagnostic (battery second-life).

Recent research efforts are increasingly focused on developing real-time diagnostic models capable of estimating both *SOC* and *SOH* without requiring a complete cycling history. Such models aim to decouple battery monitoring from the dependence on *N*, which is often unavailable or uncertain in battery second-life scenarios. The accurate determination of these internal states is particularly relevant for battery repurposing, where cells no longer suitable for high-demand applications -such as electric vehicles (EV)- can be successfully redeployed in less stringent contexts, such as stationary storage for photovoltaic systems.

Battery second-life, particularly those based on $LiFePO_4$ chemistry, are increasingly being deployed in less demanding applications where reduced capacity and partial degradation are acceptable. Typical examples include integration into stationary photovoltaic storage systems, off-grid microgrids, and low-power electric mobility platforms such as automated guided vehicles (AGVs). In these scenarios, the lower depth-of-discharge requirements and moderate cycling profiles allow partially aged batteries to continue operating efficiently. These applications benefit from the predictable voltage response and thermal stability of $LiFePO_4$ cells, making them ideal candidates for reuse in distributed energy storage frameworks. This paradigm of circular battery usage highlights the need for alternative indicators and more robust algorithms that can infer the battery's internal state from readily measurable quantities such as voltage, temperature, impedance, or current response. By enabling intelligent reuse and life extension, these approaches not only improve resource efficiency but also reduce the environmental footprint associated with lithium battery manufacturing and disposal.

Fig. 8. Experimental LiFePO4 Battery Cycling System. Simulation of a stand-alone/on-grid Photovoltaic applications.

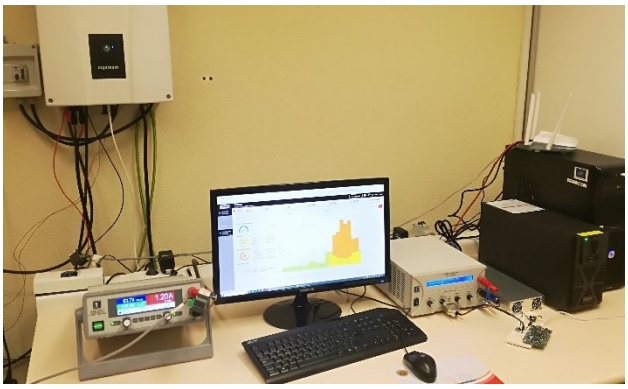

Fig. 9. Experimental setup. Power flow measurement and monitoring equipment. Estimation of electrical parameters.

TABLE I. EXPERIMENTAL MODEL DEVICES.

Description	*Manufacturer*
600W Monocrystalline Solar Panel	AutoSolar
EA-PS 3200-10C Prog. Power Supply	Elektro-Automatik
Electronic Load EA-EL 3160-60	Elektro-Automatik
Power Inverter IngeCon Sun Storage	Ingeteam
BMS Battery Box-Premium HVS	BYD
2.56kWh $LiFePO_4$ Batteries	BYD
Energy-0-RS Energy Meter Sensor	Circuitor
CEM-C21-T1 Direct Energy Meter	Circuitor

4. Experimental Battery Cycling System.

Figures 8 and 9 illustrate the experimental prototype developed to validate the behaviour of the $LiFePO_4$ battery cycling system under controlled conditions. The setup includes a photovoltaic module, a $LiFePO_4$ battery bank equipped with a Battery Management System (BMS), and a bidirectional power inverter responsible for regulating energy flows between the generation, storage, and load units. Also, a programmable power supply is integrated to emulate variable solar irradiance profiles, allowing precise replication of renewable resource fluctuations, see Table I. An active electronic load is used to simulate consumption patterns, operating in current-control mode to replicate dynamic demand scenarios.

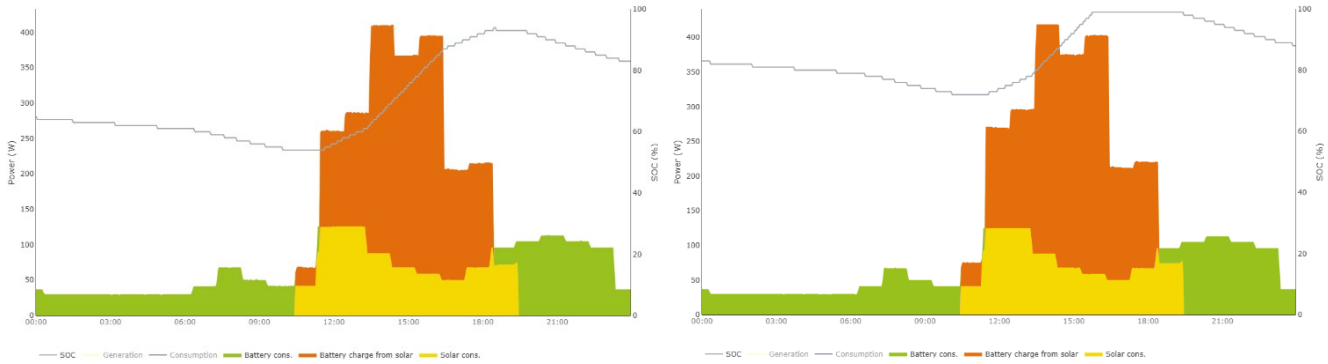

Fig. 10. Colour-map monitoring of the generated photovoltaic energy and load consumption per hour, during the days 03/27/2025 to 03/28/2025. *SOC(%)* increase of LiFePO4 battery -grey line-.

Figure 10 illustrate the power generation and consumption patterns of a $LiFePO_4$-based photovoltaic (PV) system during two consecutive days of operation. The charts provide a comprehensive visualization of solar generation, energy consumption, battery charge from solar, battery discharge, and the battery state of charge-*SOC*(%). The *SOC* curve (grey line) plays a central role in understanding system dynamics, indicating the energy stored in the battery throughout the day. On both days, PV generation starts increasing around 09:30 and reaches its peak between 13:00 and 16:00. During these hours, the energy harvested is primarily used to cover the load (yellow area) and to charge the battery (orange area), which leads to a consistent rise in *SOC*. Diagrams show a progressive charging profile, reaching approximately 90% *SOC* by late afternoon, indicating that the solar input was sufficient to replenish the battery after night-time discharge.

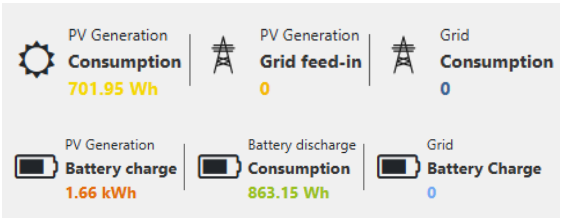

Fig. 11. Summary of the information provided by the application in real time.

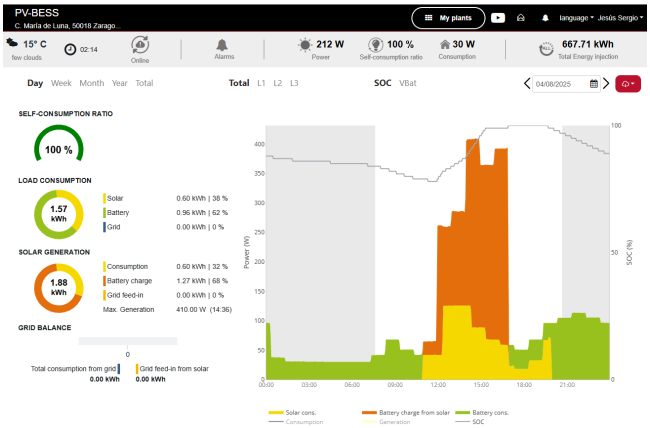

Fig. 12. PV-BESS application interface. Data and information provided in real time.

The right diagram, corresponding to the following day, reveals improved charging behaviour: the *SOC* reaches 100% approx. at 15:30. This can be attributed either to higher solar irradiance or slightly reduced system consumption during peak generation hours. Notably, battery discharging (green area) dominates during the early morning and evening periods when solar production is negligible. The consistent discharge patterns in both graphs confirm the system's ability to sustain the load during non-generating periods, while also preventing deep discharge thanks to sufficient daytime recharging. Additionally, the relatively stable consumption profile throughout both days suggests controlled and predictable demand, which supports the system's efficient battery cycling strategy.

These results highlight the balance between energy autonomy and reliability in hybrid PV-battery systems, reinforcing the viability of $LiFePO_4$ chemistry in off-grid or weak-grid applications due to its robust performance and stable *SOC* behaviour.

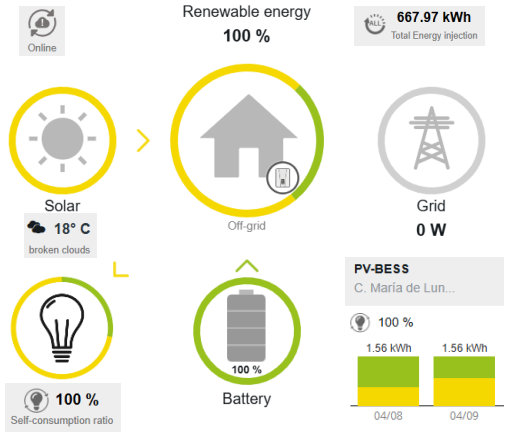

Fig. 13. Simplified diagram of the PV-BESS system.

Based on the diagrams presented, a detailed hourly energy balance of the system can be conceptualized by evaluating the power flows between solar generation, consumption, battery storage, and potential grid interaction. So, total energy balance of the system over a 24-hour period, with data sampled at 1-minute intervals, can be expressed as:

$$\sum_{i=1}^{1440} P_{PV}(i)\Delta t + \sum_{i=1}^{1440} P_{grid}(i)\Delta t = \tag{6}$$

$$= \sum_{i=1}^{1440} P_{load}(i)\Delta t + \sum_{i=1}^{1440} P_{bat}(i)\Delta t + \sum_{i=1}^{1440} P_{loss}(i)\Delta t$$

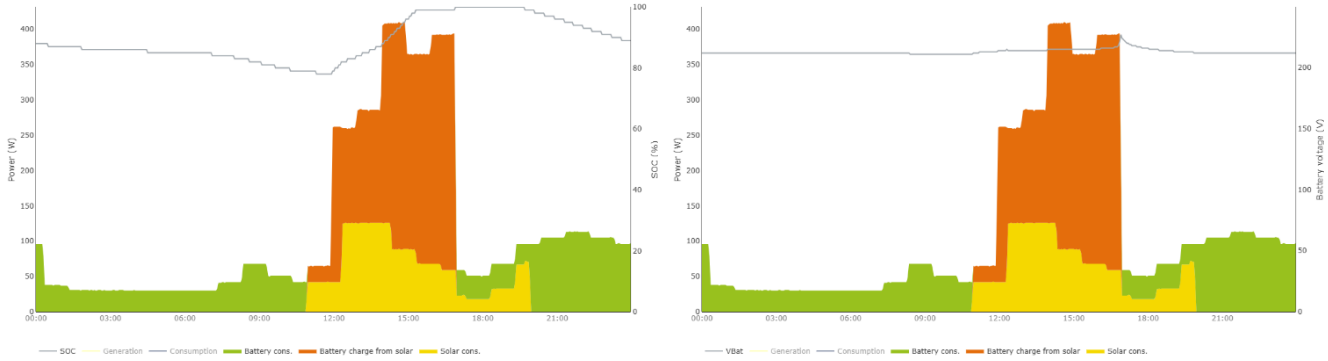

Fig. 14. Colour-map monitoring of the generated photovoltaic energy and load consumption per hour (04/08/2025). *SOC(%)* increase and voltage in LiFePO4 battery -grey line-.

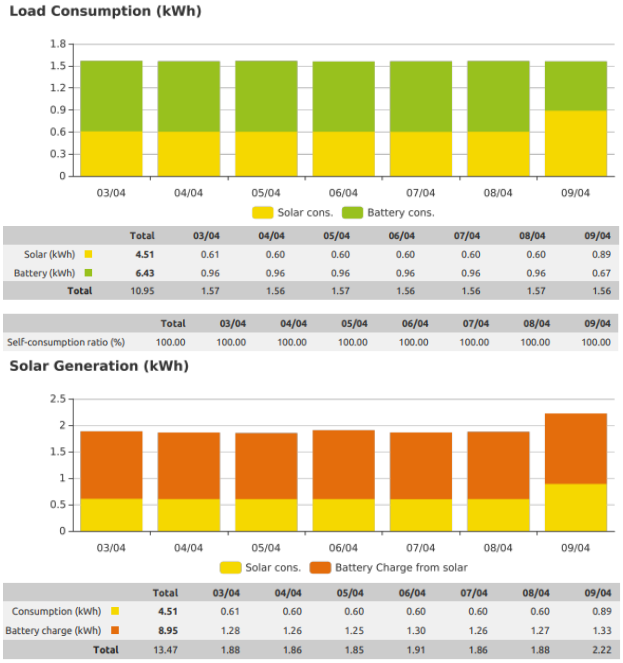

	Total	03/04	04/04	05/04	06/04	07/04	08/04	09/04
Solar (kWh)	4.51	0.61	0.60	0.60	0.60	0.60	0.60	0.89
Battery (kWh)	6.43	0.96	0.96	0.96	0.96	0.96	0.96	0.67
Total	10.95	1.57	1.56	1.57	1.56	1.56	1.57	1.56

	Total	03/04	04/04	05/04	06/04	07/04	08/04	09/04
Self-consumption ratio (%)	100.00	100.00	100.00	100.00	100.00	100.00	100.00	100.00

	Total	03/04	04/04	05/04	06/04	07/04	08/04	09/04
Consumption (kWh)	4.51	0.61	0.60	0.60	0.60	0.60	0.60	0.89
Battery charge (kWh)	8.95	1.28	1.26	1.25	1.30	1.26	1.27	1.33
Total	13.47	1.88	1.86	1.85	1.91	1.86	1.88	2.22

Fig. 15. Weekly report with the energy results of the stand-alone photovoltaic system with battery energy storage system.

where, i is minute index (from 1 to 1440, corresponding to 24 hours), and Δt corresponds to Time step = 1 minute (1/60 hour). $P_{PV}(i)$ is the power generated by the photovoltaic array at minute i (kW), $P_{grid}(i)$ represents power supplied by the electrical grid at minute i (if applicable), $P_{load}(i)$ is power consumed by the system/load at minute i, $P_{loss}(i)$ are the system losses (conversion, wiring, etc.), while $P_{bat}(i)$ represents net battery power flow at minute i. $P_{bat}>0$ during charging and $P_{bat}<0$ during discharging. Thus, the energy terms (in kWh) are computed as:

$$E = \frac{1}{60}\sum_{i=1}^{1440} P(i) \qquad (7)$$

When the battery reaches 100% state of charge (*SOC*), the system exhibits a characteristic voltage peak (Fig. 14), indicating the transition to the battery's fully charged state. At this point, the charging controller or Battery Management System (BMS) limits the current intake to prevent overcharging, resulting in a temporary increase in terminal voltage followed by a sharp drop in power absorption from the PV source. This behaviour is typical of $LiFePO_4$ battery chemistry, where the voltage plateau is followed by a rapid rise at the end of the charging cycle. Once full charge is detected, the charge controller disconnects or reduces the charging current, prioritizing direct solar-to-load supply and potentially triggering curtailment or energy diversion strategies. This protective mechanism ensures battery longevity and thermal stability while maintaining system efficiency.

5. Conclusion.

The experimental study presented in this work has validated the performance of a $LiFePO_4$ battery-based photovoltaic system under both stand-alone and on-grid scenarios, emphasizing its operational reliability, charge/discharge dynamics, and energy management efficiency. The modeling and implementation of the battery cycling system allowed precise monitoring of the *SOC* evolution, confirming the stability and responsiveness of $LiFePO_4$ chemistry under variable irradiance and load conditions. The proposed experimental setup demonstrates significant advantages in terms of energy autonomy, thermal stability, and extended cycle life, reinforcing its suitability for hybrid PV-battery configurations. Overall, the developed platform provides a replicable model for simulating and validating energy storage systems in distributed renewable applications, bridging experimental and predictive modeling.

Acknowledgement

This work was supported by the Spanish Government (Ministerio de Ciencia e Innovación, Agencia Estatal de Investigación) and by the European Regional Development Fund [Grant PID2021-123172OB-I00 funded by MCIN/AEI/10.13039/ 501100011033 and by "ERDF A way of making Europe"]

References

[1] Dufo-López, R.; Lujano-Rojas, J.M.; Artal-Sevil, J.S.; Bernal-Agustín, J.L. "Optimising Grid-Connected PV-Battery Systems for Energy Arbitrage and Frequency Containment Reserve". *Batteries, MDPI Journals. Open Access.* 2024, Vol. 10, issue: 12; pp.: 1–29.

[2] J.S. Artal-Sevil, V. Ballestín-Bernad, J.M. Lujano-Rojas, R. Dufo-López, J.L. Bernal-Agustín. "Modeling of a stand-alone solar photovoltaic water pumping system for irrigation". *Renewable Energy and Power Quality Journal (RE&PQJ).* July 2023, Vol. 21; pp.: 662–667.

[3] Huang, S.-C., Tseng, K.-H., Liang, J.-W., Chang, C.-L., & Pecht, M. G. (2017). "An Online SOC and SOH Estimation Model for Lithium-Ion Batteries". *Energies, MDPI Open Access.* 2017, vol. 10(4), 512. Pp: 1-18.